REVIEW

# Enzymatic degradation of biopolymers in amorphous and molten states: mechanisms and applications

Anđela Pustak[1] and Aleksandra Maršavelski[2] (iD)

1 Radiation Chemistry and Dosimetry Laboratory, Division of Materials Chemistry, Ruđer Bošković Institute, Zagreb, Croatia
2 Department of Chemistry, Faculty of Science, University of Zagreb, Croatia

**Correspondence**
A. Maršavelski, Department of Chemistry, Faculty of Science, University of Zagreb, Horvatovac 102a, Zagreb, Croatia
Tel: +385 1 4606 241
E-mail: amarsavelski.chem@pmf.hr

Plastic waste from fossil-derived polymers remains a major environmental challenge, driving interest in biopolymers and enzyme-enabled end-of-life strategies. This review synthesizes current understanding of how polymer structure and thermal state govern enzymatic degradability, with emphasis on semicrystalline architectures and state-dependent accessibility. Within the Keller–Flory two-phase framework, crystalline lamellae embedded in an amorphous matrix dictate water/enzyme diffusion, chain mobility, and hydrolysis kinetics. Enzymatic attack preferentially initiates in amorphous regions, producing characteristic biphasic behavior as amorphous domains erode faster than crystalline regions, leading to crystallinity enrichment and subsequent slowing of degradation. Thermal transitions further modulate this balance: near or above $T_g$, segmental mobility and free volume rise, accelerating hydrolysis if enzymes remain stable; above $T_m$, chain mobility is maximal, but enzyme stability typically limits feasibility. Processing and architecture also strongly influence outcomes: annealing increases crystallinity and slows mass loss, quenching suppresses crystallization and hastens degradation, random copolymerization disrupts packing and lowers $T_m$, while block copolymers often degrade selectively by domain. Recent advances expand the operational window toward rubbery or near-molten states for low-melting aliphatic polyesters (e.g., PCL, PLGA, PEG-$b$-PLA), leveraging thermophilic/engineered hydrolases (cutinases, PETases, lipases, carboxylesterases) with demonstrated stability at 60–90 °C. Emerging strategies—including enzyme thermostabilization, AI-guided design, disulfide grafting, smart encapsulation, and $in$-$situ$ enzyme embedding—enable self-degradation of materials and accelerate inside-out depolymerization under mild triggers. Integrating thermal analysis with polymer morphology and enzyme engineering offers a path to programmable, circular end-of-life for biopolymers, translating fundamental structure–property–reactivity relationships into practical enzymatic recycling and reduced environmental impact.

**Abbreviations**
CA, cellulose acetate; DMA, dynamic mechanical analysis; DSC, differential scanning calorimetry; DTA, differential thermal analysis; IR, infrared spectroscopy; LCC, leaf-branch compost cutinase; MW, molecular weight; NMR, nuclear magnetic resonance; PCL, poly (caprolactone); PCL-co-PLA, poly(caprolactone)-co-poly(lactic acid); PE, polyethylene; PEG-b-PLA, poly(ethylene glycol)-$b$-poly(lactic acid); PET, polyethylene terephthalate; PGA, poly(glycolic acid); PHA, poly(hydroxyalkanoate); PHB/PHBV, poly(hydroxybutyrate) (valerate); PLA, poly (lactic acid); PLGA, poly(L-lactide-$co$-glycolide); PLLA, poly(L-lactic acid); PP, polypropylene; $T_c$, crystallization temperature; $T_g$, glass transition temperature; TGA, thermogravimetric analysis; $T_m$, melting temperature; TPS, starch thermoplastic; $x_c$, degree of crystallinity; XRD, X-ray diffraction.

Plastic pollution from fossil fuel–derived materials has become a pressing environmental and public health issue, driving urgent demand for ecological and sustainable alternatives. In this context, biopolymers—materials derived from renewable natural sources—have emerged as promising substitutes for conventional fossil-based polyolefin plastics. Often referred to as bioplastics, bio-based polymers encompass a wide range of materials that are generally categorized into two groups: bio-based but non-biodegradable (43.7% of global bioplastics production in 2024) and bio-based and biodegradable (56.3%) (Fig. 1).

Global bioplastics production in 2024 is estimated at 2.5 million tonnes [1]. According to IUPAC, a biodegradable polymer is "a polymer susceptible to degradation by biological activity, with the degradation accompanied by a lowering of its molar mass" [1,2]. In practice, international legislation defines biodegradability through performance-based standards that specify: (a) required end products of degradation (e.g. $CO_2$, water, biomass, and under anaerobic conditions methane); (b) timeframes for mineralization; (c) environmental conditions—industrial composting, home composting, soil, marine, or landfill—under which

degradation must be demonstrated and (d) ecotoxicity and residue safety [3]. It is also important to distinguish compostability from biodegradability: while biodegradability refers solely to the material's capacity to mineralize through biological processes, compostability requires additional testing for physical disintegration and verification that no ecotoxic effects arise from the resulting compost.

Biopolymers—produced either by living organisms or synthesized from renewable feedstocks—are structurally and functionally diverse. They are commonly classified according to monomer chemistry, biological origin, production method, and thermal or mechanical properties [4,5]. Although the production of bioplastics is steadily increasing, matching the mechanical, thermal, rheological, and other functional properties of conventional polyolefins such as poly(ethylene) (PE), poly(propylene) (PP), and poly(ethylene terephthalate) (PET) remains a major challenge [6,7]. As a result, biopolymers are gaining market share primarily in single-use packaging applications, while traditional polyolefins continue to dominate in high-performance sectors like automotive, construction, and furniture manufacturing [1].
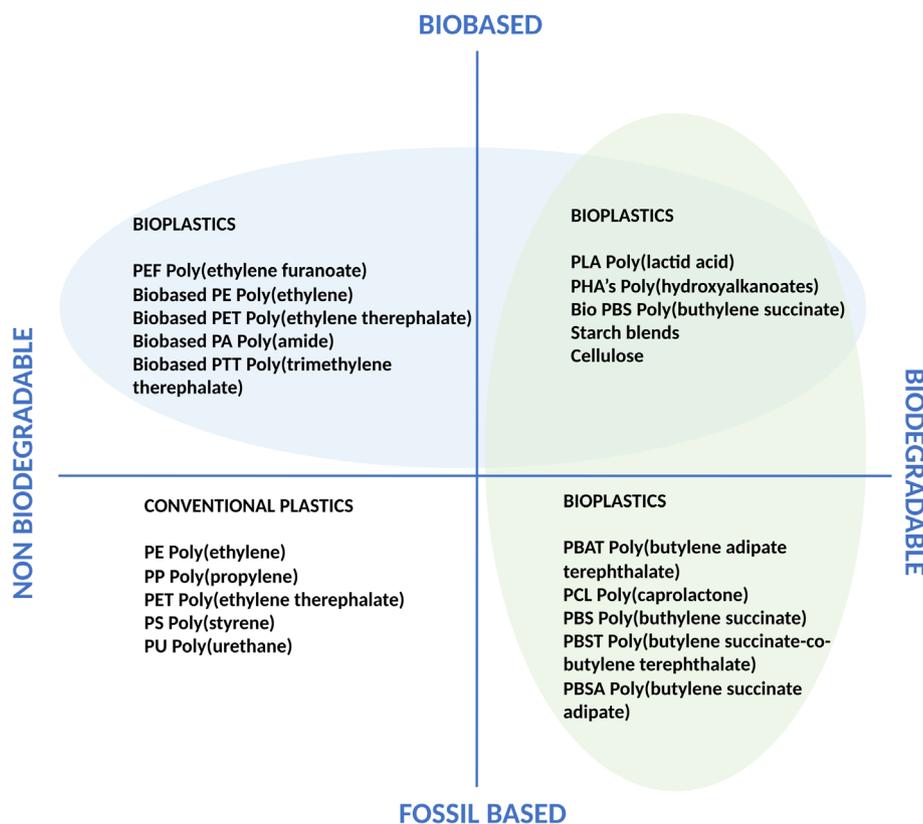


**BIOBASED**

**BIOPLASTICS**

PEF Poly(ethylene furanoate)
Biobased PE Poly(ethylene)
Biobased PET Poly(ethylene therephalate)
Biobased PA Poly(amide)
Biobased PTT Poly(trimethylene therephalate)

**BIOPLASTICS**

PLA Poly(lactid acid)
PHA's Poly(hydroxyalkanoates)
Bio PBS Poly(buthylene succinate)
Starch blends
Cellulose

**NON BIODEGRADABLE**

**BIODEGRADABLE**

**CONVENTIONAL PLASTICS**

PE Poly(ethylene)
PP Poly(propylene)
PET Poly(ethylene therephalate)
PS Poly(styrene)
PU Poly(urethane)

**BIOPLASTICS**

PBAT Poly(butylene adipate terephthalate)
PCL Poly(caprolactone)
PBS Poly(buthylene succinate)
PBST Poly(buthylene succinate-co-butylene terephthalate)
PBSA Poly(buthylene succinate adipate)

**FOSSIL BASED**

**Fig. 1.** Plastic materials classification concerning origin and biodegradability (adapted from European Bioplastics) [1].

The ever-increasing use of biopolymers highlights the urgent need to investigate degradation mechanisms—particularly microbial and enzymatic pathways—that can support sustainable waste management and enable the transition toward a circular economy.

## Polymer structure and phase states: crystalline vs. amorphous

The supermolecular architecture of semicrystalline polymers is most often explained by the *two-phase model* introduced by Keller and Flory, which describes the polymer as a system of discrete crystalline lamellae embedded within an amorphous matrix [8,9]. Each lamella consists of polymer chains that fold back and forth in a regular, three-dimensional arrangement, while the surrounding interlamellar amorphous regions contain randomly coiled and entangled chains lacking long-range order (Fig. 2).

Although the two-phase model (Fig. 2) simplifies polymer structure by considering only crystalline and amorphous phases without explicitly considering interfacial regions, it effectively captures the structural dichotomy that determines many materials' macroscopic properties—including tensile strength, barrier performance, thermal behavior, and biodegradability. The physical behavior of a polymer is thus closely tied to the relative proportions and spatial distribution of these two domains [10–12].

## Hierarchical organization and enzymatic degradation implications

The hierarchical structure of semicrystalline polymers presents substantial obstacles to enzymatic attack. Crystalline lamellae act as physical barriers that strongly restrict water and enzyme diffusion, thereby slowing or even preventing biodegradation. The densely packed crystalline cores of spherulites are particularly resistant to enzymatic attack, acting as protective shields that restrict enzyme penetration into the bulk material [6,13,14]. This structural organization amplifies the barrier effect by enclosing amorphous zones within crystalline networks, thereby limiting access to hydrolysable bonds. Consequently, enzymatic degradation is typically initiated in the more accessible amorphous regions—such as interlamellar spaces or interspherulitic boundaries—provided that enzymes can penetrate through the surrounding crystalline network. This preferential attack pattern underscores the critical importance of polymer morphology in determining biodegradation rates and pathways [13–16].

The crystallinity-to-amorphous ratio (i.e., *degree of crystallinity*) is a critical factor in determining the physical, mechanical, and degradability properties of polymers. Higher crystalline content increases density, hardness, modulus, and solvent resistance, while higher amorphous content imparts softness, elasticity, and ease of processing [17]. Although crystalline ordering in polymers has been extensively studied, amorphous regions—often described by the "bowl of spaghetti"
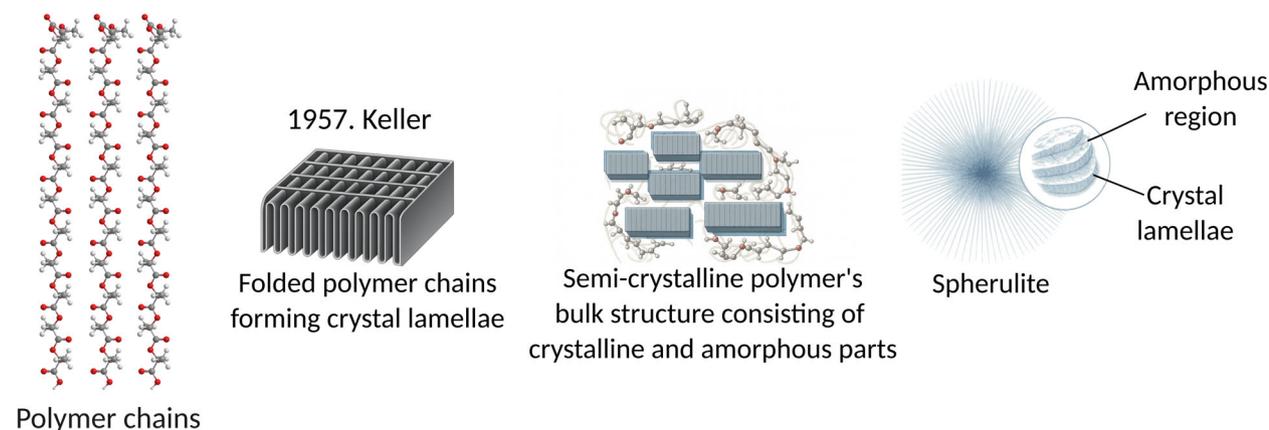
**Fig. 2.** Scheme of two-phase model describing the polymer structure. Polymer chains are folded in 10 nm thick layers called crystal lamellae that continue to grow as crystalline components. Between crystal regions, polymer chains remain unorganized, forming the amorphous component of the polymers' structure. These lamellae stack together to form crystallites – small, ordered domains where polymer chains are tightly packed in a regularly repeating structure – while the amorphous areas between lamellae, by contrast, represent disordered, non-crystalline areas [76]. The two-phase model provides the structural foundation for understanding the formation of higher-order supramolecular morphologies during polymer crystallization. Upon cooling from the melt or precipitation from a dilute solution, crystalline and amorphous regions further self-organize into complex structures such as spherulites, dendrites, or axialites [77–80].

**Table 1.** Overview of polymer states characteristics [10,20,23].

| Polymer state | Chain mobility | Structural order | Temperature range |
|---|---|---|---|
| Crystalline | Vibrational motions only | Long-range lamellar order (within crystallites) | Below melting point ($T_m$) (amorphous fraction may be glassy $<$ g or rubbery $>$ g) |
| Glassy | Localized rotations (frozen chains) | No long-range order | $\sim (T_g - 10\ K)$ to $T_g$ |
| Rubbery (viscoelastic) | Cooperative segmental motions, relaxation transition | Disordered (amorphous) | Between $T_g$ and $T_m$ |
| Melt | Whole-chain diffusion | None | $> T_m$ |

model of randomly coiled chains—are equally important for understanding degradation mechanisms. The interplay between these domains fundamentally governs enzymatic degradation: crystalline areas restrict chain mobility and enzyme access, while amorphous areas provide enhanced molecular mobility and greater accessibility, allowing enzymes to diffuse, bind, and catalyze bond cleavage more efficiently [18,19]. This structure–property relationship explains why polymers with lower crystallinity generally exhibit faster enzymatic degradation rates, while highly crystalline materials tend to be more persistent in biological environments.

## Phase states and phase transitions in polymers

Polymers exhibit complex thermal behavior characterized by distinct phase transitions that fundamentally govern their physical properties and degradation susceptibility. Three key transition temperatures define polymer behavior: the glass transition temperature ($T_g$), melting temperature ($T_m$), and crystallization temperature ($T_c$). These transitions give rise to four classical thermal states (Table 1), each reflecting different degrees of macromolecular segment mobility [20,21].

### Four thermal states of polymers

#### Crystalline state

In the crystalline solid state, polymer chains are arranged in long-range order with a highly organized lamellar structure. This dense packing significantly restricts molecular mobility, resulting in high rigidity, mechanical strength, and thermal stability. The ordered arrangement creates significant barriers to molecular diffusion, including water and enzymes.

#### Glassy state

The glassy state is characterized by disordered chain conformations that are kinetically "frozen" in place.

Although localized atomic motions may occur, the system lacks long-range mobility and exists in a metastable, non-equilibrium condition with time-dependent relaxation phenomena, including physical aging and enthalpic recovery.

#### Rubbery (viscoelastic) state

Above the glass transition temperature ($T_g$), polymers enter the rubbery state, where increased thermal energy enables greater segmental motion. Chains maintain entanglements but possess sufficient free volume to allow elastic deformation under stress [22]. This enhanced mobility significantly facilitates enzyme access to polymer backbones.

#### Melt state

Above the melting temperature ($T_m$), chain mobility becomes extensive, and the material behaves as a viscous liquid with minimal elasticity, offering theoretically optimal conditions for enzymatic attack—if enzymes can withstand the elevated temperatures [23].

#### Glass transition temperature ($T_g$)

The glass transition temperature ($T_g$) represents a second-order transition where amorphous polymer chains shift from a rigid, glassy state to a more flexible, rubbery state (Fig. 3). Unlike melting, this transition occurs gradually, without latent heat, and involves progressive changes in molecular mobility rather than an abrupt phase change (PLA as an example in Fig. 3). In semicrystalline polymers, heating beyond $T_g$ affects only the amorphous regions, while crystalline regions remain structurally intact until the melting temperature ($T_m$) is reached [10,20,23]. As temperature approaches and exceeds $T_g$, molecular mobility within amorphous regions increases dramatically. This enhanced chain dynamics facilitates enzyme diffusion and access to hydrolysable bonds, making
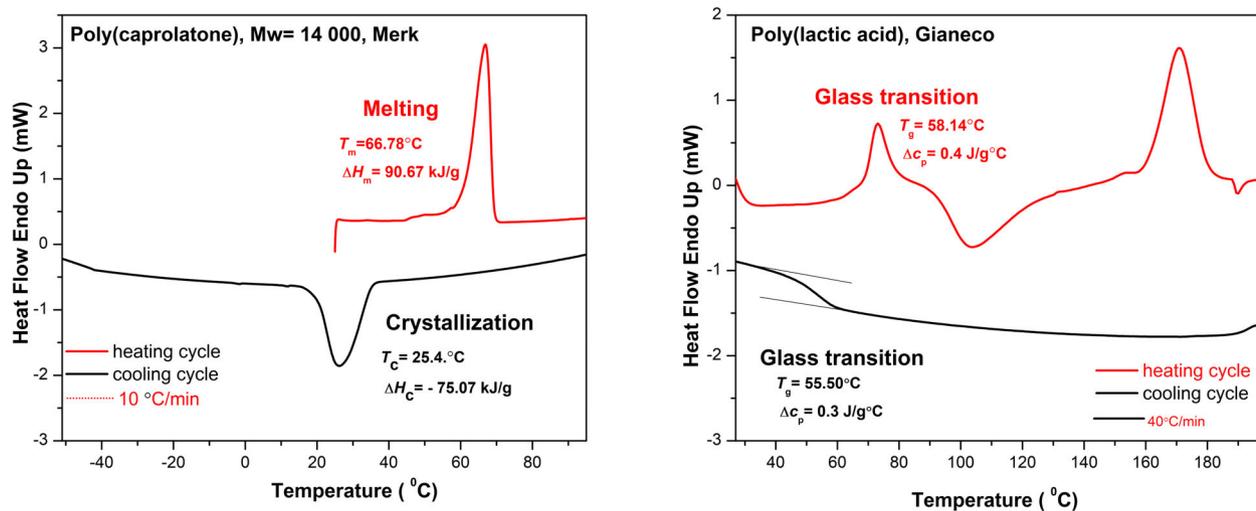
**Fig. 3.** Thermal transitions of semicrystalline polymers measured by Differential Scanning Calorimetry (DSC). Left: First-order phase transitions (melting and crystallization) of poly(ε-caprolactone) (PCL), showing melting during heating (endothermic peak corresponding to the absorption of latent heat) and crystallization during cooling (exothermic peak corresponding to the release of latent heat) at a scanning rate of 10 °C·min$^{-1}$. Right: Second-order glass transition of poly(lactic acid) (PLA) and the associated step change in heat capacity, seen as a shift in the baseline of the heat flow signal, observed during heating and cooling at 40 °C·min$^{-1}$.

the amorphous regions more susceptible to enzymatic degradation. Operating near or slightly above $T_g$ can therefore accelerate biodegradation processes, provided enzymes remain structurally stable and catalytically active under these conditions. Key factors affecting $T_g$ include tacticity, polarity, molecular weight, degree of branching or cross-linking, and the presence of additives or copolymers [20,24,25]. Understanding and controlling $T_g$ is therefore essential for designing polymers with targeted degradation profiles and predictable environmental behavior.

## Melting temperature ($T_m$)

Melting represents a first-order phase transition involving the transformation of crystalline domains into a disordered molten state. Unlike $T_g$, $T_m$ applies to the crystalline fraction and involves a sharp change in structure, accompanied by significant enthalpy changes detectable by thermal analysis methods (PCL example in Fig. 3). $T_m$ is affected by molecular geometry and symmetry, side-group interactions and polarity, molecular weight, blending or copolymerization and the degree of crystallinity [10,20,23]. At temperatures above $T_m$, polymer chains exhibit maximum mobility, theoretically offering ideal conditions for enzymatic attack [26,27]. However, most enzymes cannot withstand the thermal stress associated with elevated temperatures at or above typical polymer melting points.

## Crystallization temperature ($T_c$)

Crystallization is the reverse process of melting and occurs during cooling when polymer chains reorganize from disordered melt into ordered crystalline structures. The crystallization temperature ($T_c$) depends on chain regularity, flexibility, and intermolecular interactions, and applied cooling rate [10,20,23].

Long-range crystallization is often kinetically hindered due to chain entanglement, resulting in incomplete ordering and the formation of semicrystalline rather than fully crystalline materials.

## Crystallinity and enzymatic degradation

The degree of crystallinity ($x_c$) serves as a master variable controlling enzymatic degradation behavior. Polymers with lower crystallinity—higher amorphous content—typically degrade more rapidly under enzymatic attack due to greater chain mobility and improved accessibility to target bonds [14,27,28].

The effect becomes more evident when degradation occurs near or above $T_g$ but below $T_m$, as polymer chains are more mobile while the enzyme operates within its stability range [18,27,29]. Conversely, highly crystalline polymers, being mechanically robust and rigid and solvent-resistant, exhibit slower biodegradation. This resistance arises from the physical inaccessibility of their tightly packed, ordered domains, that severely restrict enzyme diffusion and substrate interaction.

**Table 2.** Brief overview of basic thermal techniques for biopolymer characterization [74,75].

| Thermal method – Principle | Information from method | Parameters |
| --- | --- | --- |
| Differential scanning calorimetry (DSC) – measures the difference in heat flow between a sample and a reference material as a function of temperature or time | Overall thermal stability | Temperature degradation, decomposition, oxidation |
| | First-order phase transitions such as melting and crystallization, as well as processes like cross-linking and curing | Melting temperature and enthalpy, $T_m$, $\Delta H_m$ |
| | | Crystallization temperature and enthalpy, $T_c$, $\Delta H_c$ |
| | | Degree of crystallinity, $x_c$ |
| | Second-order phase transitions—glass transition observed during both heating and cooling | Glass transition temperature, $T_g$ |
| | | Change in heat capacity $\Delta c_p$ |
| | Purity and quality control | Traces of additives, fillers, solvents, dehydration |
| Differential thermal analysis (DTA) – measures the difference in temperature between the sample and the reference material | Thermal stability especially at higher temperatures | Temperature decomposition, degradation, denaturation, oxidation |
| | Detection of melting and crystallization transitions and curing | Melting and crystallization temperature and corresponding enthalpy ($T_m$, $\Delta H_m$ $T_c$, $\Delta H_c$ less accurate than DSC) |
| | | Degree of crystallinity, $x_c$, can be estimated, though DSC is the preferred method for quantitative determination |
| | Glass transitions | Glass transition temperature, $T_g$ |
| | | Change in heat capacity $\Delta c_p$ (less accurate) |
| | Quality control | Traces of additives, fillers, solvents, dehydration |
| Thermogravimetric analysis TGA – measures the mass change of a sample as a function of temperature or time under a controlled atmosphere (commonly nitrogen for inert conditions or air/oxygen for oxidative conditions) | Thermal stability (from room temperature to high temperature) | Thermal degradation/stability, decomposition, oxidation, weight percentage, weight loss (%), $T_{onset}$ |
| | Purity information | Moisture content, solvent content and violative temperature |
| | Composition analysis and estimation of product lifetimes | Residual mass measurements, presence of substances and additives in sample |
| Dynamic mechanical analysis DMA – measures the viscoelastic properties of a material by applying a small oscillatory deformation (stress or strain) and recording the resulting dimensional/elastic response, usually as a function of temperature, time, or frequency | Thermal stability, relaxation transitions ($\alpha$, $\beta$, $\gamma$) and phase transitions (more sensitive than DSC), cross-linking, curing | Melting, crystallization, glass temperature, relaxation transition or processes in polymers (local motions of polymer groups $T_\alpha$, $T_\beta$, $T_\gamma$) |
| | Mechanical properties and behavior depend on temperature, time and frequency | Storage modulus ($E'$) |
| | | Loss modulus ($E''$) |
| | | Damping factor (tang $\delta$) |
| | Miscibility of polymers in polymer blends | Glass temperature $T_g$ from $E'$, $E''$ or tang $\delta$ data |

The degree of crystallinity is influenced by multiple structural and processing factors, including chain regularity and symmetry, molecular weight, chain flexibility, intermolecular interactions, polymer composition (random vs. block copolymers), crystallization conditions, cooling rate, thermal history and mechanical treatment [20,21,23,24,30,31]. Crystallinity is commonly quantified using complementary analytical techniques such as differential scanning calorimetry (DSC) to analyze thermal transitions and enthalpy-based crystallinity, density measurements for bulk crystallinity estimation, nuclear magnetic resonance (NMR) for molecular mobility and local order, infrared (IR) spectroscopy for conformational analysis, and X-ray diffraction (XRD) to determine crystalline vs. amorphous scattering profiles [32,33].

Given the direct impact of crystallinity on enzymatic and environmental degradation rates, accurate thermal characterization is essential for designing polymers with predictable and controllable degradation behavior (Table 2).

# Enzymatic degradation mechanisms

## Preferential degradation in amorphous regions

Enzymatic degradation of polymers preferentially occurs in amorphous regions, where increased chain
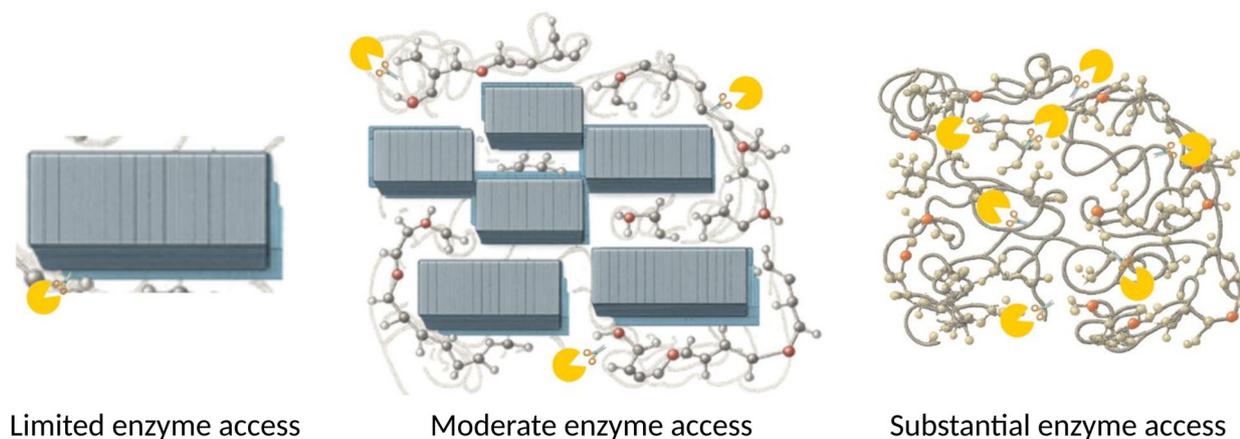
**Fig. 4.** Schematic representation of the enzymatic degradation of polymers with varying crystallinity. In highly crystalline regions, the rigid structure restricts enzyme accessibility and activity, whereas in amorphous regions with greater chain mobility, enzyme access is facilitated, leading to more efficient degradation.

mobility facilitates enzyme access and subsequent chain scission [14,28,34]. The enhanced segmental motion and greater free volume in these disordered domains allow enzymes to diffuse more readily, forming productive enzyme-substrate complexes, catalyzing bond cleavage more efficiently than in densely packed crystalline regions. However, degradation is not exclusively limited to amorphous areas. Crystalline regions can also undergo enzymatic attack [35], particularly at crystallite interfaces, grain boundaries and surface defects where structural imperfections provide enzyme and solvent access points [36]. Additionally, solvent-mediated swelling can create transient channels within crystalline domains, enabling enzyme penetration and subsequent attack (Fig. 4).

Once the enzyme gains access to the amorphous phase of the polymer, degradation proceeds efficiently. Using the depolymerization of poly(lactic acid) (PLA) as an example, enzymatic degradation occurs through a series of hydrolytic cleavage reactions catalyzed at the ester bonds along the polymer backbone. The process involves a nucleophilic attack on the carbonyl carbon, leading to bond cleavage and progressive depolymerization into shorter oligomers and, ultimately, lactic acid monomers (Fig. 5). This schematic representation illustrates the stepwise hydrolysis mechanism and highlights the catalytic role of the enzyme in facilitating PLA chain breakdown.

Recent advances in protein engineering have revealed the importance of conformational selectivity in enzymatic polymer degradation. Notably, engineered PETase variants from *Ideonella sakaiensis*, have been tailored to preferentially bind the trans-conformation of PET, which is enriched in crystalline domains [37]. This conformational selection proves critical for enzymatic activity: trans-selective PETase variants exhibited enhanced hydrolysis of crystalline PET due to improved substrate-enzyme compatibility. Remarkably, even single amino acid substitutions were sufficient to reshape the enzyme's conformational landscape, promoting more productive binding geometries and significantly increasing catalytic efficiency toward trans conformers within ordered crystalline regions in PET [37]. This demonstrates the potential pathway for rational enzyme design to overcome the long-standing limitations of crystalline polymer degradation.

## Impact of polymer architecture on enzymatic degradation

Polymer architecture – whether a material exists as a homopolymer, random copolymer, or block copolymer (Table 3) – significantly influences enzymatic degradation behavior, and represents a key design parameter for controlling biodegradation rates. Random copolymer incorporation generally increases enzymatic degradability because the irregular monomer sequence disrupts crystal packaging, reduces overall crystallinity and lowers $T_m$ [18,38]. For instance, random copolymerization has proven effective for enhancing enzymatic degradation rate of succinate-based polymers [39], where the incorporation of different diol or dicarboxylic acid comonomers reduces crystallinity and accelerates biodegradation. The irregular chain structure prevents efficient packing of polymer chains, resulting in materials with predominantly amorphous character that are more susceptible to enzymatic attack. Block copolymers exhibit fundamentally
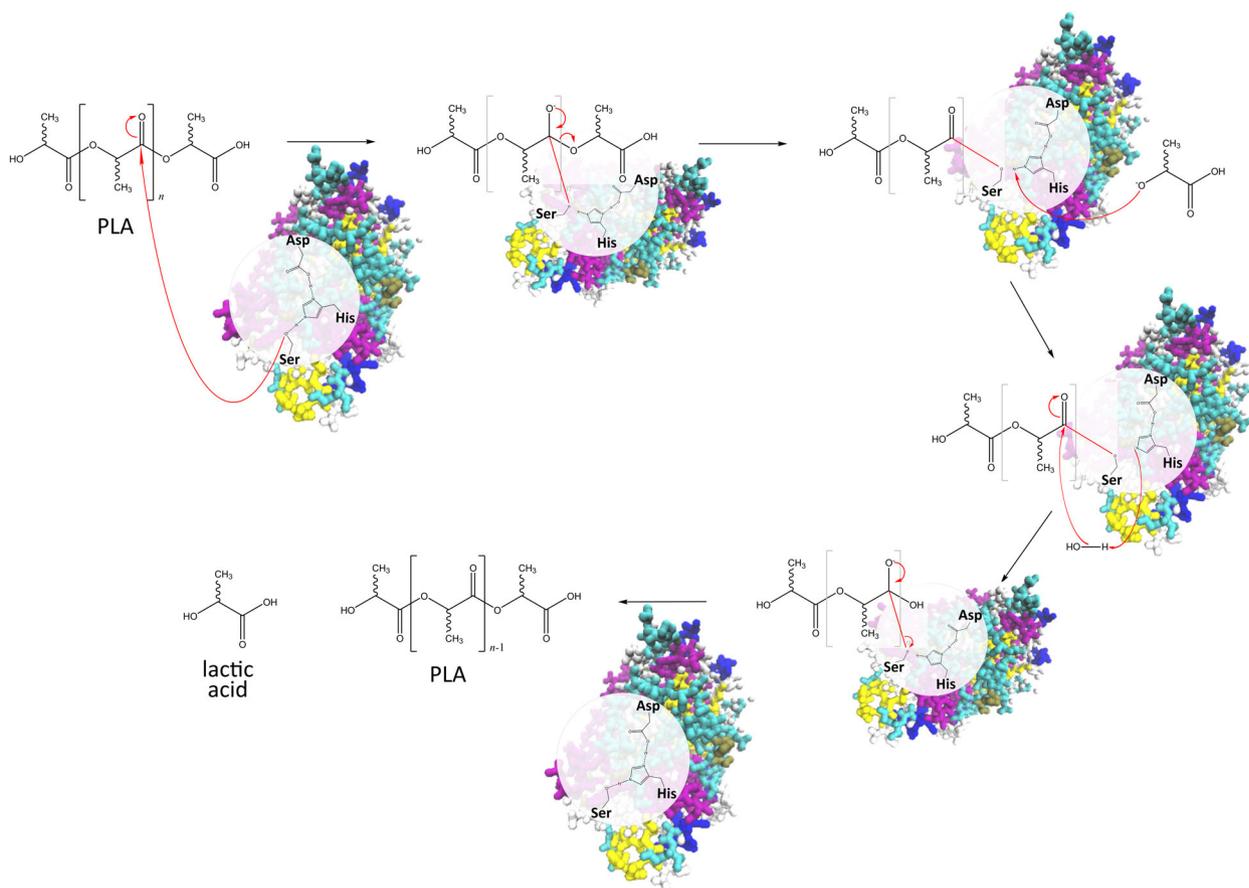
**Fig. 5.** Proposed enzymatic degradation mechanism of poly(lactic acid) (PLA) catalyzed by a polyester hydrolase. The reaction proceeds via a typical serine-hydrolase mechanism involving the catalytic triad (Ser-His-Asp). The enzyme's nucleophilic serine residue attacks the carbonyl carbon of the ester bond in the PLA backbone, forming a tetrahedral intermediate, which subsequently collapses to yield an acyl–enzyme intermediate and a shortened polymer chain. In the following step, a water molecule—activated by histidine—performs a nucleophilic attack on the acyl–enzyme complex, regenerating the free enzyme and releasing the hydrolyzed product. Repeated cycles of these reactions result in progressive chain-end scission and depolymerization of PLA into lactic acid monomers. The scheme illustrates the catalytic steps and the role of the enzyme's active site in facilitating ester bond cleavage.

different degradation behavior compared to their random counterparts. Block copolymers (e.g., PLA-*b*-PCL or PEG-*b*-PLA) typically phase-separate into distinct domains (blocks) with different chemical and physical properties. This phase separation leads to selective enzymatic degradation, where enzymes may preferentially attack one block while leaving the other largely intact. For instance, in PEG-*co*-PLA block copolymers, Proteinase K primarily targets PLA segments while PEG regions remain essentially unchanged [40].

## Enzymatic degradation in the amorphous regions

A paradigmatic example is the degradation of poly(3-hydroxybutyrate) (PHB) by extracellular PHB depolymerase from *Alcaligenes faecalis* T1. This enzyme initially hydrolyzes PHB chains in amorphous surface regions before gradually eroding the remaining crystalline domains. Kumagai *et al.*, [41] reported that the enzymatic hydrolysis rate of PHB films decreases proportionally with increasing crystallinity, as enzymes must either await spontaneous loosening of amorphous-crystalline interfaces or actively induce structural disruption before accessing crystalline chains. Importantly, crystalline spherulites' size showed minimal impact on degradation rates, while the fraction of crystallinity proved decisive —low-crystallinity PHB films degraded substantially faster than high-crystallinity counterparts under identical conditions.

Poly(lactic acid) (PLA) exhibits similar crystallinity-dependent degradation, existing in both amorphous (primarily poly(D,L-lactide)) and

**Table 3.** Commonly used commercial biopolymers and block copolymers, along with their molecular structures, degree of crystallinity ($X_c$), and thermal parameters—melting temperature ($T_m$), crystallization temperature ($T_c$), and glass transition temperature ($T_g$)—representing the thermal window relevant for polymer targeting [18,49–53,74].
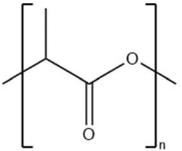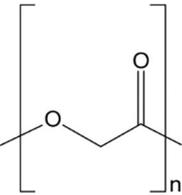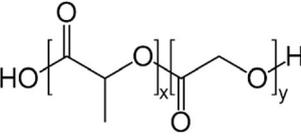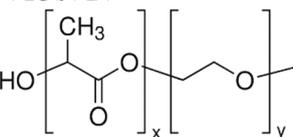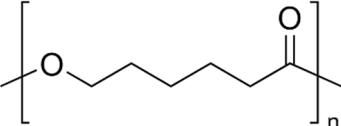
| Biopolymer | Degree of crystallinity $w_{cx}$ (%) | $T_m$ (°C) | $T_c$ (°C) | $T_g$ (°C) |
|---|---|---|---|---|
| Poly(lactic acid) (PLA)  | 10–40 | 150–180 | 80–130 | 55–65 |
| Poly(glycolic acid) (PGA)  | 45–55 | 225–230 | 140–180 | 30–40 |
| Poly(L-lactide-co-glycolide) (PLGA) (50/50)  | 0–10 (Amorphous) | 135–155 | – | 45–55 |
| Poly(ethylene glycol)-b-poly(lactid acid) PEG-b-PLA  | Depends on block length and $M_w$ | 40–55 (PEG) 150–170 (PLA) | 40–60 (PEG) 80–130 (PLA) | −60 (PEG) 55 (soft blocks of PLA) 40–55 (hard block of PLA) |
| Poly(hydroxyalkanoate) (PHA)  | 30–70 | 160–180 | 60–90 | −10 to 5 |
| Poly(hydroxybutyrate) (valerate) (PHB/PHBV)  | 50–70 | 170–180 | 80–100 | 5–10 |
| Poly(caprolactone) (PCL)  | 40–60 | 58–64 | 30–40 | −60 |
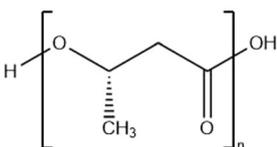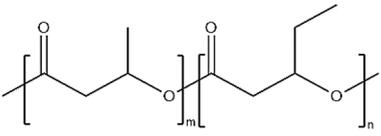
**Table 3.** (Continued).

| Biopolymer | Degree of crystallinity $w_{cx}$ (%) | $T_m$ (°C) | $T_c$ (°C) | $T_g$ (°C) |
|---|---|---|---|---|
| Poly(caprolactone)-*co*-Poly(lactic acid) PCL-*co*-PLA | ~ 20–30 (PCL) ~ 20 (PLA) in 50/50 copolymer | 60–110 | ~ 30 (PLC) | −40 to 10 |
| Starch thermoplastic (TPS) | 0–30 | – | Broad peak | −50 to 20 |
| Cellulose acetate (CA) | 0–20 | – | Broad peak | 170–190 |
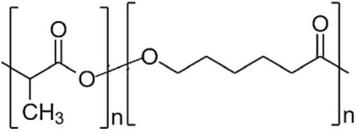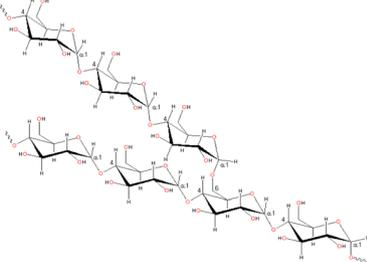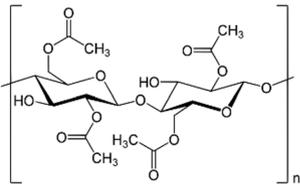
semicrystalline variants (poly(L-lactide)) [34,42]. In semicrystalline PLA, enzymatic and hydrolytic degradation begins in amorphous domains, where water penetration and enzymes drive rapid molecular weight loss [34,43]. This preferential attack creates a characteristic biphasic degradation pattern. The first stage is rapid, targeting accessible amorphous regions. As amorphous domains are selectively removed, the material undergoes "crystallinity enrichment" phenomenon—not through new crystal formation, but through selective depletion of the amorphous phase [44,45]. The remaining crystalline-rich material exhibits substantially reduced degradation rates, often requiring additional environmental triggers such as elevated temperatures, or prolonged exposure to mechanical stress to disrupt crystalline order for continued enzymatic degradation.
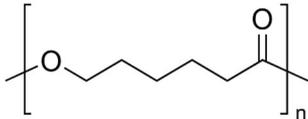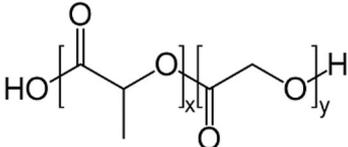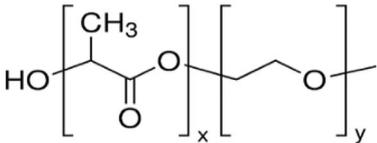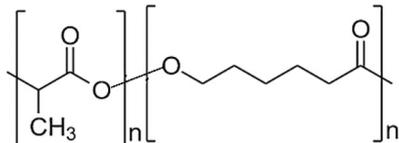
Thermal pretreatment effects [46] demonstrate clear structure–property relationships. Annealing, which increases crystallinity through controlled heating, significantly reduces degradation rates, while rapid cooling (quenching) suppresses crystallization and enhances amorphous content, thereby accelerating degradation under both enzymatic and hydrolytic conditions [1,47].

# Enzymatic degradation in the molten (or near-molten) state of low-melting biopolymers

Certain biopolymers and copolymers possess relatively low melting points including poly(ε-caprolactone) (PCL, $T_m \approx 60$ °C), [48] poly(lactic acid-*co*-glycolic acid) (PLGA, many PLGA compositions are amorphous, showing only glass transition temperatures $\approx 31–60$ °C, [47] depending on LA : GA ratio), [49] poly(ethylene glycol)-*b*-polylactide (PEG-*b*-PLA), [50] poly(ε-caprolactone-*co*-lactide) (PCL-co-PLA) [51] making them suitable candidates for studying enzymatic activity under molten-state conditions (Table 4). The combination of (i) polymers with melting temperatures ($T_m$) between 45 and 120 °C and (ii) thermophilic or engineered enzymes that maintain activity within this thermal window unlocks a previously inaccessible frontier in biocatalytic recycling: enzymatic depolymerization in the rubbery or fully molten state.

The relatively low melting temperatures of certain aliphatic polyesters, such as PCL [48] and low-crystallinity PLA, [42] enable polymer chain mobility that approaches small-molecule liquid behavior at temperatures where many thermostable enzymes retain

**Table 4.** Thermal window of the target polymers, presented graphically for selected examples [48–51].

| Polymer | $T_g$ (°C) | $T_m$ (°C) | Notes | Polymer (typical composition) |
|---|---|---|---|---|
| PCL (ε-caprolactone) | −60 | 55–62 | Fully molten at mild temperatures—ideal test bed | PCL (ε-caprolactone) |
| PLGA | ≈ −5 to 15 | 135–155 | $T_g$ only slightly above ambient; partial melting starts ≈ 130 °C | PLGA (50 : 50) |
| PEG-b-PLA | −60 (PEG)/ 55–60 (PLA) | 40–55 (soft block)/150–170 (hard block) | Microphase-separated: soft PEG melts < 50 °C | PEG-b-PLA (MW ≈ 2 kDa/ 5 kDa) |
| PCL-co-PLA | −40 to 10 | 60–110 (broad) | $T_m$ depressed relative to neat PLA, enabling "semi-molten" states at 70–90 °C | PCL-co-PLA (random, 50 : 50) |

activity, creating opportunities for molten-state enzymatic depolymerization that would be impossible with high-melting-point polymers like PET without highly specialized enzyme variants.

Several natural and engineered lipases, esterases, and polyester hydrolases exhibit remarkable thermostability and catalytic efficiency near the glass transition temperature of PET (≈ 70 °C). Among them, the thermophilic cutinase variant Leaf-Branch Compost Cutinase (LCC[ICCG]) shows a melting temperature of ≈ 92 °C and maintains high depolymerization activity at 68 °C, achieving nearly complete (≈ 98%) PET conversion within 24 h while remaining stable throughout the reaction [52]. The hyperthermostable alkaline lipase from *Bacillus sonorensis* 4R exhibited optimal activity at 80 °C and retained a half-life ($t_{1/2}$) of 150 min at this temperature [53] and hyperthermophilic carboxylesterases from extremophilic archaea, such as the *Pyrococcus furiosus* esterase, remain properly folded and catalytically active at 100 °C, exhibiting optimal activity at this temperature and retaining a half-life of 34 h at 100 °C and 50 min at 126 °C [54,55]. Beyond naturally robust enzymes, protein

engineering has dramatically expanded biocatalyst thermal tolerance. Recent advances in AI-driven enzyme engineering, ancestral sequence reconstruction (ASR), and structure-guided stabilization strategies have markedly enhanced the thermostability of PET hydrolases. Using machine learning algorithms, such as MutCompute, researchers have identified mutations that optimize local residue environments and enhance folding robustness, yielding highly stable variants like FAST-PETase that efficiently depolymerize untreated post-consumer PET at 50 °C [56]. In parallel, ancestral sequence reconstruction approaches have reconstructed ancient hydrolase ancestors of *Ideonella sakaiensis* PETase, uncovering stabilizing mutations distant from the active site that increase melting temperatures by up to 20 °C while retaining or improving catalytic activity [57]. Complementary strategies, including SpyTag/SpyCatcher cyclization to improve conformational rigidity [58] and rational disulfide bridge incorporation, have further reinforced enzyme stability. Collectively, these methods have produced engineered PETases and cutinases—such as HotPETase, DuraPETase, LCC[ICCG], and newly evolved PET2-21 M—with
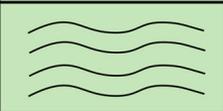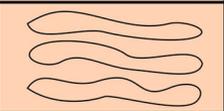
# How Molten-State Mobility Shapes

| | Solid-state (below $T_g$) | Rubbery ($T_g \rightarrow T_m$) | Molten (> $T_m$) |
|---|---|---|---|
| **Chain mobility** | | | |
| **Water uptake** | Low | Moderate | High (if emulsified) |
| **Enzyme adsorption** | Surface-limited | Surface + shallow penetration | Potential 3-D access via convective mixing |
| **Expected mode** | Surface erosion | Mixed erosion / bulk | True bulk depolymerisation (if enzyme survives) |

**Fig. 6.** Schematic illustrating how polymer state governs enzymatic depolymerization. As polymers transition from solid (below $T_g$) to rubbery ($T_g \rightarrow T_m$) and molten (> $T_m$), chain mobility and water uptake increase, shifting enzyme action from surface-limited erosion to mixed erosion/bulk degradation—and, when molten and emulsified, enabling 3-D access via convective mixing for true bulk depolymerization (if the enzyme remains stable).

melting temperatures ranging from 80 °C to nearly 99 °C, maintaining high catalytic efficiency under industrially relevant conditions [59–62].

The physical state of polymers relative to their thermal transitions fundamentally determines enzymatic degradation pathways. Below $T_g$, in the glassy state, polymer chains remain essentially immobilized with minimal water uptake and enzyme interaction limited to surface adsorption, resulting in surface erosion [63]. In the rubbery regime between $T_g$ and $T_m$, enhanced segmental chain motion and improved water absorption enable shallow enzyme penetration, creating a hybrid of surface and limited bulk degradation [63]. In the molten state (above $T_m$), extensive chain mobility permits free polymer diffusion, significantly enhanced water uptake, particularly in emulsified systems, and potential three-dimensional enzyme access through convective mixing, enabling true bulk depolymerization provided enzymes maintain structural and catalytic stability at elevated temperatures (Fig. 6). This mechanistic understanding of state-dependent degradation patterns provides crucial insights for designing next-generation enzymatic recycling processes that can exploit the enhanced accessibility of molten or near-molten polymer states while maintaining enzyme functionality through strategic thermostabilization approaches [64].

## Future perspective and conclusion

Most enzymes face significant thermal limitations that prevent direct depolymerization of fully molten polymers, as materials like PLA melt at $\approx$ 150–170 °C, far exceedingly even the most thermostable enzyme stability ranges. This thermal incompatibility has traditionally restricted enzymatic degradation to solid state conditions, limiting exploitation of enhanced chain mobility in molten states. However, emerging strategies are bridging this gap through innovative protein engineering and materials science approaches.

Thermostable enzyme development represents a critical breakthrough, exemplified by recent advances in PETase and cutinase engineering [65]. The wild-type IsPETase enzyme [66,67] has been engineered into a variant known as HotPETase, which features a significantly enhanced melting temperature of approximately 82.5 °C. Additionally, a naturally occurring cutinase from leaf-branch compost (LCC) has been engineered to exhibit a $T_m$ of about 94 °C [61]. On the industrial side, Carbios, a French biotechnology company, has progressed toward commercializing enzymatic PET recycling. They are constructing the world's first industrial-scale PET biorecycling plant in Longlaville, France, which upon completion will have the capacity to process roughly 50 000 tonnes of post-consumer PET waste per year.

*In-situ* enzyme incorporation into plastics represents perhaps the most revolutionary approach. DelRe *et al.*, [68] presented a breakthrough approach to plastic waste management through nano-dispersed enzyme embedding, where enzymes are incorporated as nanoparticles (< 2% by weight) directly into semicrystalline polyesters during manufacturing to create self-degrading materials. The key innovation involves using protective polymer complexes that maintain enzyme stability during high-temperature processing while enabling activation upon water exposure, leading to processive depolymerization. The results demonstrate up to 98% polymer-to-small-molecule conversion within days for poly(caprolactone) and poly(lactic acid) in standard soil composts and household tap water, with complete elimination of microplastic formation due to the chain-end-mediated degradation mechanism.

Building upon this foundation, Guicherd *et al.*, [69] developed a commercially viable PLA-based plastic with embedded hyperthermostable PLA hydrolase, achieving an 80-fold activity enhancement through structure-based rational engineering and demonstrating full disintegration under home-compost conditions within 20–24 weeks using only 0.02% w/w enzyme loading. Their scalable masterbatch-based melt extrusion process involved incorporating the liquid enzyme formulation into polycaprolactone at 70 °C, then integrating these masterbatch pellets into PLA at 160 °C, producing enzymatic films that maintain mechanical properties compatible with industrial packaging applications while ensuring rapid biodegradation at room temperature.

Computational and machine learning–guided methods are rapidly accelerating enzyme optimization [56,70], markedly reducing development timelines from years to mere months. For instance, Shao *et al.*, [71] introduced EnzyHTP, a high-throughput computational platform that integrates adaptive resource management with directed evolution strategies to efficiently model and refine enzyme variants *in silico*. Meanwhile, the PRIME language model [72], a temperature-aware deep learning framework, has demonstrated the ability to predict single- and multi-site mutations that enhance protein stability and activity—over 30% of AI-suggested mutants outperformed their wild-type counterparts without experimental mutagenesis. These approaches are part of a broader wave of advances in computational protein design—including Nobel-recognized efforts [73]—highlighting the transformative power of AI in rapidly designing enzymes with improved thermostability and substrate specificity.

Future research is prioritizing circular economy integration by designing enzymatic recycling pathways that yield high-value monomers suitable for direct repolymerization. The EU's Horizon Europe program has invested €2.4 billion in enzymatic recycling technologies, while industrial partnerships between companies like Carbios, Eastman, and major brands demonstrate approaching commercial viability.

This review demonstrates that enzyme-mediated polymer degradation has evolved from fundamental research to practical applications. The integration of advanced enzyme engineering with a sophisticated understanding of polymer thermal behavior is creating opportunities for truly circular systems where biodegradation becomes an integral design feature, promising high-performing materials that completely biodegrade when their service life concludes—a critical step toward sustainable polymer waste management and environmental impact reduction.

## Acknowledgements

## Conflict of interest

The authors declare no conflict of interest.

## Author contributions

AP and AM contributed equally to the work. Their roles included conceptualization, investigation and literature search, writing of the original draft, review and editing of the manuscript, and preparation of visualizations.

## References

1 Bioplastics market development update 2024 – european bioplastics. https://www.european-bioplastics.org/bioplastics-market-development-update-2024/

2 The IUPAC Compendium of Chemical Terminology (2025) https://goldbook.iupac.org/.

3 Kim MS, Chang H, Zheng L, Yan Q, Pfleger BF, Klier J, Nelson K, Majumder ELW and Huber GW (2023) A

review of biodegradable plastics: chemistry, applications, properties, and future research needs. *Chem Rev* **123**, 9915–9939.

4 Chen GQ and Patel MK (2012) Plastics derived from biological sources: present and future: a technical and environmental review. *Chem Rev* **112**, 2082–2099.

5 Mohan S, Oluwafemi OS, Kalarikkal N, Thomas S, Songca SP, Mohan S *et al.* (2016) Biopolymers – application in nanoscience and nanotechnology. In *Recent Advances in Biopolymers* (Perveen F, ed.), Vol. **1**, pp. 47–66. InTechOpen, London, UK.

6 Siddiqui SA, Yang X, Deshmukh RK, Gaikwad KK, Bahmid NA and Castro- R (2024) Recent advances in reinforced bioplastics for food packaging – a critical review. *Int J Biol Macromol* **263**, 130399-421.

7 Huang S, Dong Q, Che S, Li R and Tang KHD (2025) Bioplastics and biodegradable plastics: a review of recent advances, feasibility and cleaner production. *Sci Total Environ* **969**, 178911.

8 Keller A (1957) A note on single crystals in polymers: evidence for a folded chain configuration. *Philos Mag* **2**, 1171–1175.

9 Flory PJ (1962) On the morphology of the crystalline state in polymers. *J Am Chem Soc* **84**, 2857–2867.

10 Tager A (1972) *Physical Chemistry of Polymers*. Mir, Moscow, Russia.

11 Strobl GR and Schneider M (1980) Direct evaluation of the electron density correlation function of partially crystalline polymers. *J Polym Sci Polym Phys Ed* **18**, 1343–1359.

12 Wunderlich B (1973) *Crystal Structure, Morphology, Defects In Macromolecular Physics*. Academic Press INC, London, UK.

13 Suresh V, Shams R, Dash KK, Shaikh AM and Béla K (2025) Comprehensive review on enzymatic polymer degradation: a sustainable solution for plastics. *J Agric Food Res* **20**, 101788.

14 Spyros A, Kimmich R, Briese BH and Jendrossek D (1997) 1H NMR imaging study of enzymatic degradation in poly(3-hydroxybutyrate) and poly(3-hydroxybutyrate-co-3-hydroxyvalerate). Evidence for preferential degradation of the amorphous phase by PHB depolymerase B from pseudomonas lemoignei. *Macromolecules* **30**, 8218–8225.

15 Tournier V, Duquesne S, Guillamot F, Cramail H, Taton D, Marty A and André I (2023) Enzymes' power for plastics degradation. *Chem Rev* **123**, 5612–5701.

16 Samir A, Ashour FH, Hakim AAA and Bassyouni M (2022) Recent advances in biodegradable polymers for sustainable applications. *NPJ Mater Degrad* **6**, 1–28.

17 Nielsen EL (1962) *Mechanical Properties of Polymers*. Van Nostrand Reinhold Corp, New York, USA. pp. 137–212

18 Schwab ST, Bühler LY, Schleheck D, Nelso n TF and Mecking S (2024) Correlation of enzymatic depolymerization rates with the structure of polyethylene-like long-chain aliphatic polyesters. *ACS Macro Lett* **13**, 1245–1250.

19 Wei R, Breite D, Song C, Gräsing D, Ploss T, Hille P, Schwerdtfeger R, Matysik J, Schulze A and Zimmermann W (2019) Biocatalytic degradation efficiency of postconsumer polyethylene terephthalate packaging determined by their polymer microstructures. *Adv Sci* **6**, 1900491.

20 Wunderlich B (2005) *Thermal Analysis of Polymeric Materials*. Springer, New York, NY. pp. 279–450

21 Campbell D, Pethrick RA and White JR (2001) *Polymer Characterization: Physical Techniques*. Second edn. CRC Press, London, UK. pp. 1–481

22 Saito S and Nakajima T (1959) Glass transition in polymers. *J Appl Polym Sci* **2**, 93–99.

23 Seymour RB and Carraher CE (1984) Thermal properties of polymers. In *Structure—Property Relationships in Polymers* pp. 83–93. Springer, Boston, USA.

24 Müller AJ and Michell RM (2016) Differential scanning calorimetry of polymers. In *Polymer Morphology: Principles, Characterization, and Processing* (Guo Q, ed.), pp. 72–99. Wiley Book, NY, USA.

25 Menczel JD, Judovits L, Prime RB, Bair HE and Swier S (2014) Differential Scanning Calorimetry (DSC). In *Thermal Analysis of Polymers: Fundamentals and Applications* (Menczel DJ and Prime RB, eds), pp. 1–704. Wiley, USA.

26 Azevedo HS and Reis RL (2004) *Understanding the enzymatic degradation of biodegradable polymers and strategies to control their degradation rate in biodegradable Systems in Tissue Engineering and Regenerative Medicine* (Reis, RL, Román, JS, eds). CRC Press, Taylor and Francis Group, UK. pp. 177–202

27 Thomsen TB, Hunt CJ and Meyer AS (2022) Influence of substrate crystallinity and glass transition temperature on enzymatic degradation of polyethylene terephthalate (PET). *New Biotechnol* **69**, 28–35.

28 He Y, Shuai X, Kasuya KI, Doi Y and Inoue Y (2001) Enzymatic degradation of atactic poly(R,S-3-hydroxybutyrate) induced by amorphous polymers and the enzymatic degradation temperature window of an amorphous polymer system. *Biomacromolecules* **2**, 1045–1051.

29 Lippold H, Kahle L, Sonnendecker C, Matysik J and Fischer C (2022) Temporal and spatial evolution of enzymatic degradation of amorphous PET plastics. *Npj Mater Degrad* **6**, 1–6.

30 Mandelkern L (1985) The relation between structure and properties of crystalline polymers. *Polym J* **17**, 337–350.

31 Nojima S, Fujimoto M, Kakihira H and Sasaki S (1998) Effects of copolymer composition on the

crystallization and morphology of poly(ε-caprolactone)-block-polystyrene. *Polym J* **30**, 968–975.

32 Saalwächter K, Thurn-Albrecht T and Paul W (2023) Recent Progress in understanding polymer crystallization. *Macromol Chem Phys* **224**, 2200424.

33 Murthy NS and Minor H (1990) General procedure for evaluating amorphous scattering and crystallinity from X-ray diffraction scans of semicrystalline polymers. *Polymer* **31**, 996–1002.

34 Shalem A, Yehezkeli O and Fishman A (2024) Enzymatic degradation of polylactic acid (PLA). *Appl Microbiol Biotechnol* **108**, 1–20.

35 Kaabel S, Daniel, Therien JP, Deschênes CE, Duncan D, Friščić T and Auclair K (2021) Enzymatic depolymerization of highly crystalline polyethylene terephthalate enabled in moist-solid reaction mixtures. *Proc Natl Acad Sci USA* **118**, e2026452118.

36 Ong A, Teo JYQ and Lim JYC (2024) Interfacial reactions in chemical recycling and upcycling of plastics. *ACS Appl Mater Interfaces* **16**, 46975–46987.

37 Guo B, Vanga SR, Lopez-Lorenzo X, Saenz-Mendez P, Ericsson SR, Fang Y et al. (2022) Conformational selection in biocatalytic plastic degradation by PETase. *Acs Catalysis* **12**, 3397–3409.

38 Michelle RM, Müller AJ, Castelletto V, Hamley I, Deshayes G and Dubois P (2009) Effect of sequence distribution on the morphology, crystallization, melting, and biodegradation of poly(ε-caprolactone-co-ε-caprolactam) copolymers. *Macromolecules* **42**, 6671–6681.

39 Bi S, Tan B, Soule JL and Sobkowicz MJ (2018) Enzymatic degradation of poly (butylene succinate-co-hexamethylene succinate). *Polym Degrad Stab* **155**, 9–14.

40 He M, Hsu YI and Uyama H (2024) Superior sequence-controlled poly(L-lactide)-based bioplastic with tunable seawater biodegradation. *J Hazard Mater* **474**, 134819.

41 Kumagai Y, Kanesawa Y and Doi Y (1992) Enzymatic degradation of microbial poly(3-hydroxybutyrate) films. *Die Makromolekulare Chemie* **193**, 53–57.

42 Zaaba NF and Jaafar M (2020) A review on degradation mechanisms of polylactic acid: hydrolytic, photodegradative, microbial, and enzymatic degradation. *Polym Eng Sci* **60**, 2061–2075.

43 Kumar A, Weig AR and Agarwal S (2022) Balancing degradability and physical properties of amorphous poly(d,l-lactide) by making blends. *Macromol Mater Eng* **307**, 2100602.

44 Peñas MI, Beloqui A, Martínez de Ilarduya A, Suttiruengwong S, Hernández R and Müller AJ (2024) Enzymatic degradation behavior of self-degradable lipase-embedded aliphatic and aromatic polyesters and their blends. *Biomacromolecules* **25**, 4030–4045.

45 Polińska M, Rozanski A, Galeski A and Bojda J (2021) The modulus of the amorphous phase of Semicrystalline polymers. *Macromolecules* **54**, 9113–9123.

46 Ciuffi B, Fratini E and Rosi L (2024) Plastic pretreatment: the key for efficient enzymatic and biodegradation processes. *Polym Degrad Stab* **222**, 110698.

47 Pantani R and Sorrentino A (2013) Influence of crystallinity on the biodegradation rate of injection-moulded poly(lactic acid) samples in controlled composting conditions. *Polym Degrad Stab* **98**, 1089–1096.

48 Bartnikowski M, Dargaville TR, Ivanovski S and Hutmacher DW (2019) Degradation mechanisms of polycaprolactone in the context of chemistry, geometry and environment. *Prog Polym Sci* **96**, 1–20.

49 Park K, Otte A, Sharifi F, Garner J, Skidmore S, Park H, Jhon YK, Qin B and Wang Y (2021) Potential roles of the glass transition temperature of PLGA microparticles in drug release kinetics. *Mol Pharm* **18**, 18–32.

50 Soo XYD, Muiruri JK, Yeo JCC, Png ZM, Sng A, Xie H, Ji R, Wang S, Liu H, Xu J et al. (2023) Polyethylene glycol/polylactic acid block co-polymers as solid–solid phase change materials. *SmartMat* **4**, e1188.

51 Botlhoko OJ, Ramontja J and Ray SS (2018) A new insight into morphological, thermal, and mechanical properties of melt-processed polylactide/poly(ε-caprolactone) blends. *Polym Degrad Stab* **154**, 84–95.

52 Arnal G, Anglade J, Gavalda S, Tournier V, Chabot N, Bornscheuer UT, Weber G and Marty A (2023) Assessment of four engineered PET degrading enzymes considering large-scale industrial applications. *ACS Catal* **13**, 13156–13166.

53 Bhosale H, Shaheen U and Kadam T (2016) Characterization of a Hyperthermostable alkaline lipase from *Bacillus sonorensis* 4R. *Enzyme Res* **2016**, 4170684.

54 Levisson M, van der Oost J and Kengen SWM (2009) Carboxylic ester hydrolases from hyperthermophiles. *Extremophiles* **13**, 567–581.

55 Ikeda M and Clark DS (1998) Molecular cloning of extremely thermostable esterase gene from hyperthermophilic archaeon *Pyrococcus furiosus* in *Escherichia coli*. *Australas Biotechnol* **57**, 624–629.

56 Lu H, Diaz DJ, Czarnecki NJ, Zhu C, Kim W, Shroff R, Acosta DJ, Alexander BR, Cole HO, Zhang Y et al. (2022) Machine learning-aided engineering of hydrolases for PET depolymerization. *Nature* **604**, 662–667.

57 Joho Y, Vongsouthi V, Spence MA, Ton J, Gomez C, Tan LL, Kaczmarski JA, Caputo AT, Royan S, Jackson CJ et al. (2023) Ancestral sequence reconstruction identifies structural changes underlying the evolution of *Ideonella sakaiensis* PETase and variants with improved stability and activity. *Biochemistry* **62**, 437–450.

58 Hayes HC and Luk LYP (2023) Investigating the effects of cyclic topology on the performance of a plastic degrading enzyme for polyethylene terephthalate degradation. *Sci Rep* **13**, 1–11.

59 Sana B, Ding K, Siau JW, Pasula RR, Chee S, Kharel S, Lena JBH, Goh E, Rajamani L, Lam YM *et al.* (2023) Thermostability enhancement of polyethylene terephthalate degrading PETase using self- and nonself-ligating protein scaffolding approaches. *Biotechnol Bioeng* **120**, 3200–3209.

60 Matsuzaki T, Saeki T, Yamazaki F, Koyama N, Okubo T, Hombe D, Ogura Y, Hashino Y, Tatsumi-Koga R, Koga N *et al.* (2025) Development and production of moderate-thermophilic PET hydrolase for PET bottle and fiber recycling. *ACS Sustain Chem Eng* **13**, 10404–10417.

61 Tournier V, Topham CM, Gilles A, David B, Folgoas C, Moya-Leclair E, Kamionka E, Desrousseaux ML, Texier H, Gavalda S *et al.* (2020) An engineered PET depolymerase to break down and recycle plastic bottles. *Nature* **580**, 216–219.

62 Zeng W, Li X, Yang Y, Min J, Huang JW, Liu W, Niu D, Yang X, Han X, Zhang L *et al.* (2022) Substrate-binding mode of a thermophilic PET hydrolase and engineering the enzyme to enhance the hydrolytic efficacy. *ACS Catal* **12**, 3033–3040.

63 Thomsen TB, Almdal K and Meyer AS (2023) Significance of poly(ethylene terephthalate) (PET) substrate crystallinity on enzymatic degradation. *New Biotechnol* **78**, 162–172.

64 Guo RT, Li X, Yang Y, Huang JW, Shen P, Liew RK and Chen CC (2024) Natural and engineered enzymes for polyester degradation: a review. *Environ Chem Lett* **22**, 1275–1296.

65 Bhattacharya S, Castagna R, Estiri H, Upmanis T, Ricci A, Gautieri A and Parisini E (2025) Development of a highly active engineered PETase enzyme for polyester degradation. *FEBS J* 70228. doi: 10.1111/febs.70228

66 Yoshida S, Hiraga K, Takehana T, Taniguchi I, Yamaji H, Maeda Y *et al.* (1979) A bacterium that degrades and assimilates poly(ethylene terephthalate). *Science* **351**, 1196–1199.

67 Bell EL, Smithson R, Kilbride S, Foster J, Hardy FJ, Ramachandran S, Tedstone AA, Haigh SJ, Garforth AA, Day PJR *et al.* (2022) Directed evolution of an efficient and thermostable PET depolymerase. *Nature Catalysis* **5**, 673–681.

68 DelRe C, Jiang Y, Kang P, Kwon J, Hall A, Jayapurna I, Ruan Z, Ma L, Zolkin K, Li T *et al.* (2021) Near-complete depolymerization of polyesters with nano-dispersed enzymes. *Nature* **592**, 558–563.

69 Guicherd M, Ben Khaled M, Guéroult M, Nomme J, Dalibey M, Grimaud F, Alvarez P, Kamionka E, Gavalda S, Noël M *et al.* (2024) An engineered enzyme embedded into PLA to make self-biodegradable plastic. *Nature* **631**, 884–890.

70 Dauparas J, Anishchenko I, Bennett N, Bai H, Ragotte RJ, Milles LF *et al.* (1979) Robust deep learning–based protein sequence design using ProteinMPNN. *Science* **378**, 49–56.

71 Shao Q, Jiang Y and Yang ZJ (2023) EnzyHTP computational directed evolution with adaptive resource allocation. *J Chem Inf Model* **63**, 5650–5659.

72 Jiang F, Li M, Dong J, Yu Y, Sun X, Wu B, Huang J, Kang L, Pei Y, Zhang L *et al.* (2024) A general temperature-guided language model to design proteins of enhanced stability and activity. *Sci Adv* **10**, 2641.

73 Howes L (2024) Baker, Hassabis, and jumper win 2024 Nobel prize in chemistry. *Chem Eng News* **102**, 4.

74 Turi EA (1997) *Thermal Characterization of Polymeric Materials*. 2nd edn. Academic Press, USA.

75 Guigo N and Sbirrazzuoli N (2018) Thermal analysis of biobased polymers and composites. In *Handbook of Thermal Analysis and Calorimetry* (Vyazovkin S, Koga N and Schick C, eds), Vol. **6**, pp. 399–429. Elsevier,

76 Ledwith A and North AM (1975) *Molecular Behaviour and the Development of Polymeric Materials*. Chapman and Hall, London, UK.

77 Lovinger AJ (2020) Twisted crystals and the origin of banding in Spherulites of Semicrystalline polymers. *Macromolecules* **53**, 741–745.

78 Li L, Chan CM, Yeung KL, Li JX, Ng KM and Lei Y (2001) Direct observation of growth of lamellae and spherulites of a semicrystalline polymer by AFM. *Macromolecules* **34**, 316–325.

79 Hoffman JD, John I and Lauritzen J (1961) Crystallization of bulk polymers with chain folding: theory of growth of lamellar Spherulites. *J Res Natl Bur Stand A Phys Chem* **65A**, 336.

80 Tashiro K, Yoshioka T, Yamamoto H, Wang H, Woo EM, Funaki K and Murase H (2019) Relationship between twisting phenomenon and structural discontinuity of stacked lamellae in the spherulite of poly(ethylene adipate) as studied by the synchrotron X-ray microbeam technique. *Polym J* **51**, 131–141.